



Water splitting on Rhodamine-B dye sensitized Co-doped TiO₂ catalyst under visible light

Thi Thu Le ^{a,1}, M. Shaheer Akhtar ^{a,b,1}, Dong Min Park ^a, Jang Choon Lee ^c, O-Bong Yang ^{a,b,*}

^a School of Semiconductor and Chemical Engineering & Solar Energy Research Center, Chonbuk National University, Jeonju 561-756, Republic of Korea

^b New & Renewable Energy Materials Development Center (NewREC), Chonbuk National University, Republic of Korea

^c Department of Infrastructure Civil Engineering, Chonbuk National University, Jeonju 561-756, Republic of Korea

ARTICLE INFO

Article history:

Received 4 June 2011

Received in revised form 14 October 2011

Accepted 16 October 2011

Available online 20 October 2011

Keywords:

TiO₂ nanoparticles

Rhodamine B dye

Dye sensitization

Photocatalyst

Water splitting

ABSTRACT

An effective rhodamine B (Rh B) dye sensitized Co doped TiO₂ (Co/TiO₂) materials was prepared by simple physical absorption for photocatalytic water splitting under visible light. The prepared Rh B-Co/TiO₂ materials showed a strong absorbance edge band in the range of 450–600 nm (max. absorbance at 550 nm) and estimated a moderate band gap of 2.58 eV, which lowered than that of Co/TiO₂ (2.75 eV). Rh B-Co/TiO₂ catalysts showed the high activity towards photocatalytic water splitting under visible light irradiation. The reaction with Rh B-Co/TiO₂ catalysts achieved a nearly stoichiometric evolution of H₂ and O₂ evolution of ~227.3 μmol/g-catal/h and ~98.9 μmol/g-catal/h, respectively, which is 6 times higher than that of H₂ evolution (~37.67 μmol/g-catal/h) over Co/TiO₂ catalysts. The enhanced water splitting reaction may be facilitated by the absorbed Rh B near to Co atom. This synergic effect between the Rh B and Co is crucial to the water splitting reaction.

© 2011 Elsevier B.V. All rights reserved.

1. Introduction

Water splitting to produce hydrogen and oxygen under visible light radiation will be one of the promising hydrogen production methods because of its cheap production cost, if it is successfully developed the active photocatalysts under visible light. The energy storage capacity of H₂ per gram (119,000 J/g) is three times larger than the storage capacity of oil (40,000 J/g). Expensive and highly sophisticated technologies such as petroleum and steam methane reforming processes are popular for the hydrogen production in large scale [1,2]. Based on one report, water electrolysis process covers only 5% of the commercial hydrogen, while most of hydrogen production (95%) is still covered by reforming of fossil fuels [3]. Contrary, the photocatalytic water splitting process is extensively studied for the hydrogen production from the decomposition of water under UV/visible light illumination in the presence of inorganic semiconducting materials [4,5]. Recently, Domen's group demonstrated reasonably high H₂ gas evolution (16.2 mmol in 35 h) from pure water with gallium and zinc nitrogen oxide catalysts

(Ga_{1-x}Zn_x)(N_{1-x}O_x) under visible light [6]. In order to find the suitable visible light active catalysts, the large band gap semiconductor materials coupled with to narrow energy band gap semiconductors and doping metals or nonmetals are possibly extend the absorption edge in visible region [7–10]. In our previous work, Yang et al. prepared a hydrothermally synthesized platinum doped titania nanotubes as visible active catalysts and exhibited moderate H₂ evolution of 14.6 μmol/h from water under visible light [11]. To enhance the visible light harvesting efficiency, dye sensitization on semiconductor materials has been recently studied for hydrogen production from water [12,13]. TiO₂ nanomaterials are one of the most popular and interesting semiconductor oxides for photocatalytic water splitting due to its high catalytic, photostability, chemical stability and nontoxic nature [14]. However, its large band gap energy (3.2 eV) limits the utilization in the photocatalytic water splitting under visible light irradiation [15].

Recently, TiO₂ and metal doped TiO₂ nanomaterials have been sensitized by various dyes such as Eosin Y [16], merocyanine [17], Ru(bpy)₃²⁺ [18] and coumarin [19] for hydrogen evolution under visible light. Subramanian et al. has investigated the photocatalytic activity of Co-doped TiO₂ films under visible illumination [20], but the Co-doped TiO₂ has not shown reasonable photocatalytic activity for water splitting to produce H₂ and O₂. However, rhodamine B (Rh B) is one of the important representations of xanthene dyes and well known as a dye laser material for its good stability [21]. In this paper, we have prepared Co doped TiO₂ nanomaterials by impregnation method and sensitized by Rh-B for photo-catalytic

* Corresponding author at: School of Semiconductor and Chemical Engineering & Solar Energy Research Center, Chonbuk National University, Jeonju 561-756, Republic of Korea. Tel.: +82 63 270 2313; fax: +82 63 270 2306.

E-mail addresses: shaheerakhtar@jbnu.ac.kr (M.S. Akhtar), obyang@jbnu.ac.kr (O.-B. Yang).

¹ These authors contributed equally to this work.

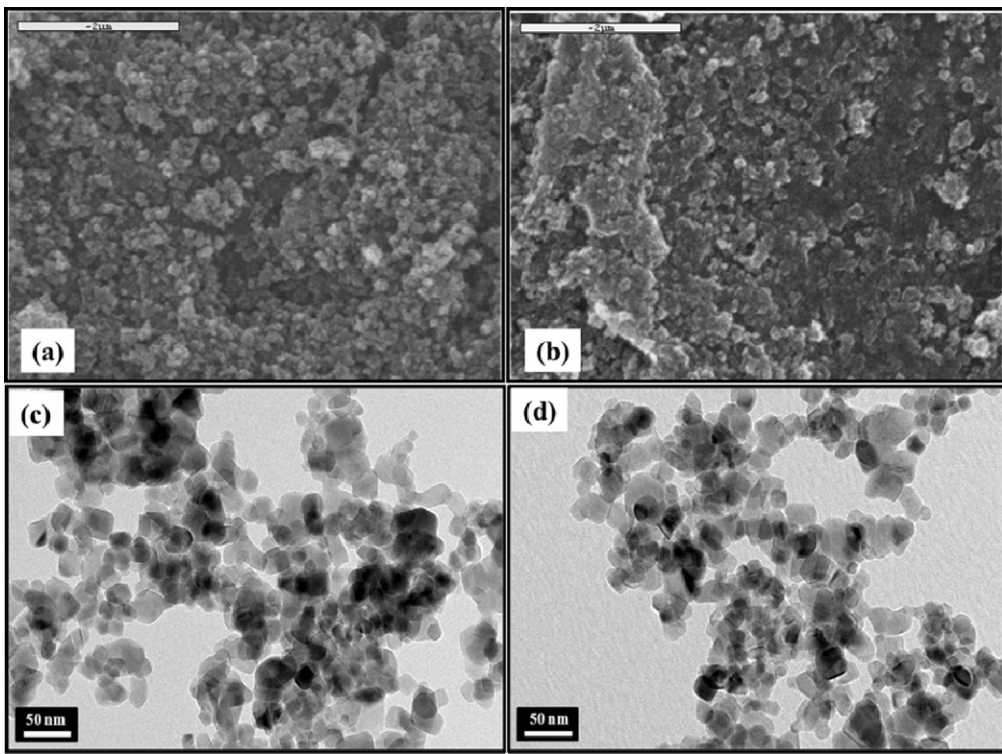


Fig. 1. SEM (a and b) and TEM (c and d) images of Co/TiO₂ (a and c) and Rh B-Co/TiO₂ (b and d), respectively.

water splitting of pure water under visible light. There is no report on the photocatalytic water splitting over the RhB-Co/TiO₂ under visible light irradiation. The photocatalytic water splitting results shows that Rh B-Co/TiO₂ materials confers a highly active in visible light to evolve the stoichiometric H₂ (~227.3 μmol/g-catal/h) and O₂ (~98.9 μmol/g-catal/h) gases from the pure water, respectively.

2. Experimental

The Co doped TiO₂ catalysts were prepared by impregnation method with TiO₂ powders (P-25, Degussa) and Co(NO₃)₂·9H₂O as precursors [22]. The desired amount of TiO₂ powder was suspended in distilled water and various amounts of Co(NO₃)₂·9H₂O (0.1 M, Aldrich Chemical analytical grade) were added. Then, the suspension was stirred at room temperature for 1 h and evaporated to dry at 80 °C. After washing several times by distilled water to remove unbound cobalt, the Co doped TiO₂ sample was calcined at 450 °C for 2 h, which denoted as Co/TiO₂. For the preparation of Rh B dye sensitized Co/TiO₂, the Rh B dye was absorbed on Co/TiO₂ (1 g) in a mixture of Rh B (1 mmol) and 70 ml of DEA (15% (v/v)) – water solution at room temperature for overnight in the dark [23]. The dye-absorbed sample was washed by acetone and dried at 40 °C under N₂ atmosphere under dark. Thus, the prepared sample denoted as Rh B-Co/TiO₂.

The prepared catalysts were characterized by X-ray diffraction (XRD) using a Rigaku diffractometer with Cu K α radiation (40 kV, 30 mA, scan speed at 6° min⁻¹ and the range of 20–80°), scanning electron microscope (SEM, JEOL-JSM 6400, Japan), transmission scanning microscopy (TEM, JEOL, JEM – 2010), Raman Spectroscopy (RFS-100S, Germany) and ultraviolet-visible diffuse reflectance spectroscopy (UV-vis DRS, Shimadzu-UV3600).

Photocatalytic water splitting experiment was carried out in an outer irradiation Pyrex cell under visible light. The Rh B-Co/TiO₂ catalyst powder (50 mg) was dispersed in 70 ml of pure H₂O solution by a magnetic stirrer and an ultrasonic bath for 10 min. A reaction suspension was purged and bubbled by ultra-pure argon

gas until no detectable dissolved oxygen in the solution before starting the reaction by visible light illumination. The visible light source used ozone-free Xe arc lamp (300 W, Hamamatsu: L 2479) attached with UV cut filter (FSQ-GC 400). The evolved amount of H₂ and O₂ were analyzed by gas chromatography (GC) equipped with a thermal conductivity detector (TCD) and a molecular sieve 5 Å column (stainless steel, 6 ft × 1/8" OD, Ar as carrier gas). The desorption of RhB dye was carried out by collecting the 2 ml of mixture solution from the water splitting reactor and then measured absorbance of collected samples by the UV-Vis spectrophotometer (Shimadzu-UV3600).

3. Results and discussion

The surface morphologies of Co/TiO₂ and Rh B-Co/TiO₂ are characterized by SEM and TEM as shown in Fig. 1. Co/TiO₂ (Fig. 1 a and c) exhibits small spherical particles with size of 20–25 nm. There are no significant differences in the morphology and size of TiO₂ and Co metal clusters after introducing Rh B on Co/TiO₂ as shown in Fig. 1(b and d). The composition of prepared catalysts is examined by electron dispersive X-ray spectrometer (EDS) coupled in scanning electron microscope (SEM) and the result is summarized in Table 1. The amount of Co metal before (1.52 wt%) and after (1.46 wt%) Rh B dye absorption is very similar, indicating that Rh B dye does not affect the morphology of Co/TiO₂.

XRD patterns of TiO₂, Co/TiO₂ and Rh B-Co/TiO₂ catalysts are shown in Fig. 2. TiO₂ (P25) possesses typically both anatase and rutile phases with 2θ peaks at 25.2, 27.4, 36.2, 37.7, 41.3, 48.0,

Table 1
Summary of EDX analysis of Co/TiO₂ and RhB-Co/TiO₂ photocatalyst.

| Elements (wt%) | Co/TiO ₂ | RhB-Co/TiO ₂ |
|----------------|---------------------|-------------------------|
| C | – | 2.24 |
| Ti | 58.64 | 55.24 |
| O | 39.84 | 41.06 |
| Co | 1.52 | 1.46 |

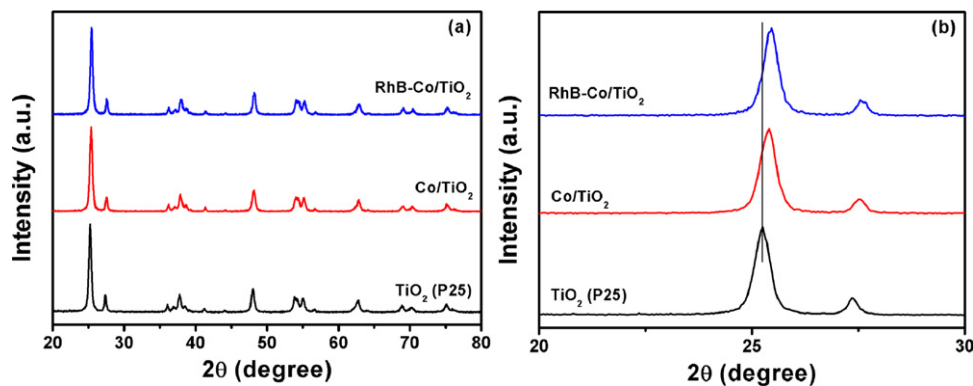


Fig. 2. The broad scale (a) and (b) small scale XRD patterns of bare TiO_2 , Co/TiO_2 and $\text{RhB-Co}/\text{TiO}_2$ catalysts.

53.8, 55.0, 56.7, 62.6, 68.8 and 75.1°. The XRD peaks are significantly shifted by 0.2° from their original position after doping of Co into TiO_2 as shown in Fig. 2(b). However, there are no XRD peak and TEM image corresponding to Co metal clusters and cobalt oxide, indicating that the most of Co is substituted to the Ti lattice site without any aggregation of Co metal clusters on exterior TiO_2 surface. This Co substitution phenomenon has been reported elsewhere [24]. $\text{RhB-Co}/\text{TiO}_2$ exhibits the similar XRD patterns of Co/TiO_2 , which suggests that RhB dye absorption does not affect the phases of Co/TiO_2 . Thus, the slight shifting in XRD peak clearly indicates the Co doping into the TiO_2 nanomaterials.

Fig. 3 shows UV-vis diffuse reflectance spectra (UV-vis DRS) of Co/TiO_2 and $\text{Rh B-Co}/\text{TiO}_2$ catalysts. Co/TiO_2 reveals an absorption edge shifting towards the lower energy region, corresponding to higher wavelength side of the spectra in the visible range (Fig. 3). However, the $\text{Rh B-Co}/\text{TiO}_2$ catalyst shows a longer shift with the strong peak in the wavelength of 500–600 nm, which indicates the absorption of Rh B dye on Co/TiO_2 catalyst. The absorption edge of Co/TiO_2 is at ~450 nm, which corresponds to band gap energy of 2.75 eV. Whereas $\text{Rh B-Co}/\text{TiO}_2$ reveals a band gap of 2.58 eV, which is significantly lower than those of Co/TiO_2 and TiO_2 (3.2 eV). These results are comparable to reported studies on metal-doped TiO_2 catalysts [25,26]. The reduction potential of Co^{2+}/Co (−0.27 V at 25 °C) is more positive than that of TiO_2 conduction band energy level (−0.52 V) [27]. Thus, the electrons transfer from the conduction band of TiO_2 to the Co^{2+} ion suppresses the back electron transfer reaction with the holes in the valence band of TiO_2 , which cause the low stoichiometric efficiency in the most of

photo-catalytic reaction. Additionally, Co^{2+} is a colored ion, which acts as a chromophore and can easily absorb light in the visible range [28] and Rh B dye sensitization on Co/TiO_2 may be enhanced the light absorption and leads the high light harvesting efficiency in the visible region as compared to TiO_2 and Co/TiO_2 catalyst. Fig. 4(a) shows the amount of absorbed Rh B dye on Co/TiO_2 as a function of dye absorption time. The Rh B dye absorption on the surface of Co/TiO_2 increases as increasing the time and reaches equilibrium to ~25.06 $\mu\text{mol-Rh B/g-catal}$ after 24 h.

Fig. 5 presents the accumulated hydrogen and oxygen evolution from pure water solution containing suspensions of bare TiO_2 , Co/TiO_2 and $\text{Rh B-Co}/\text{TiO}_2$ under visible light irradiation ($\lambda \geq 420 \text{ nm}$)

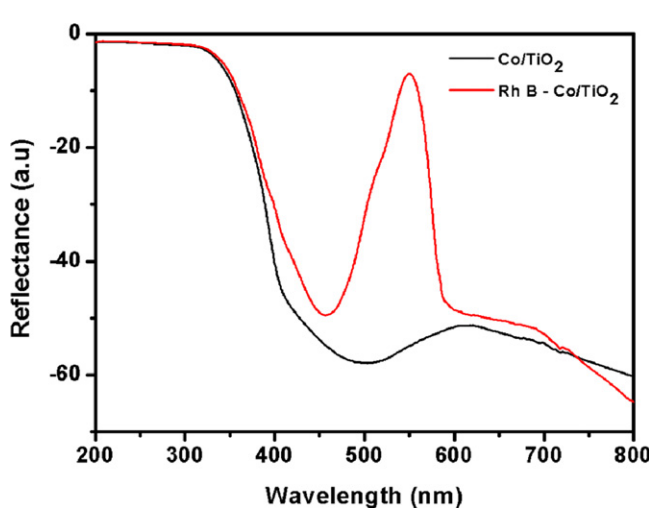


Fig. 3. UV-vis DRS of Co/TiO_2 and $\text{Rh B-Co}/\text{TiO}_2$ catalysts.

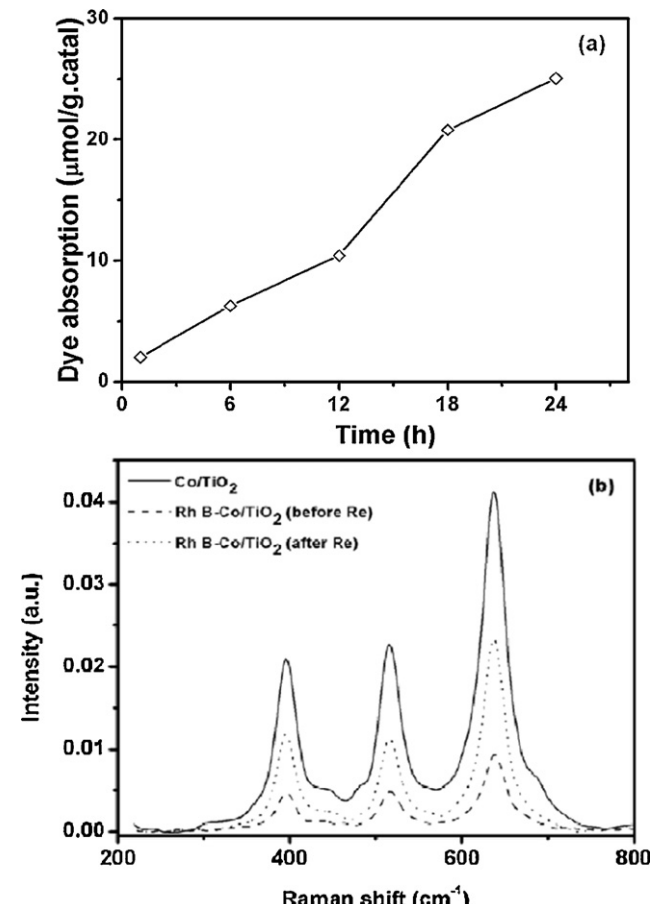


Fig. 4. (a) The rate of Rhodamine B dye absorbed on the surface of Co/TiO_2 catalyst and (b) Raman spectra of Co/TiO_2 , $\text{Rh B-Co}/\text{TiO}_2$ materials before and after reaction.

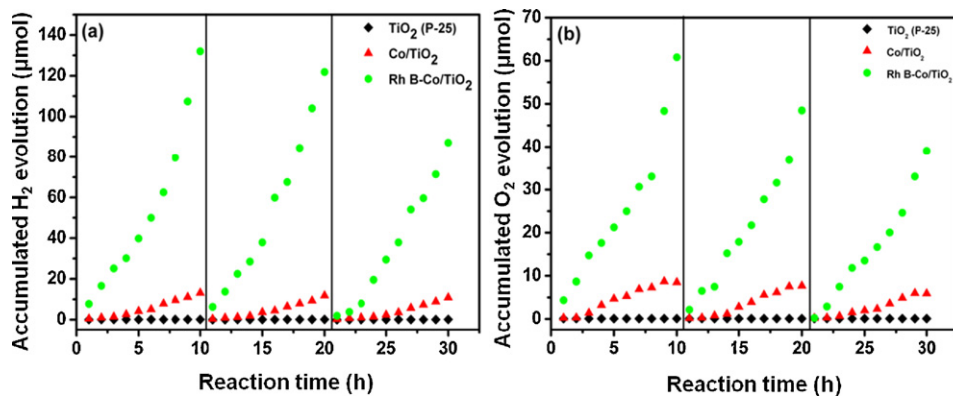


Fig. 5. (a) Accumulated hydrogen and (b) oxygen evolution as a function of reaction time over Rh B-Co/TiO_2 , Co/TiO_2 and TiO_2 photocatalysts.

with respect to reaction time and summarizes in Table 2. Rh B-Co/TiO_2 catalyst obtains significantly high rates of accumulated H_2 and O_2 evolution of ~ 227.3 ($\mu\text{mol/g-catal/h}$) and ~ 98.9 ($\mu\text{mol/g-catal/h}$), respectively, which shows a nearly stoichiometric ratio of gas evolution from water. When the light turns off, no H_2 and O_2 evolution observe, indicating that the reaction is induced by the absorption of visible light and not by any tribological or mechanical processes. Moreover, the photocatalytic reaction of water splitting has been performed with only Rh B under visible light, which shows no H_2 and O_2 production, indicating that RhB dye needs a supportive surface for generating the reduction sites of water splitting under visible light irradiation. With RhB-Co/TiO_2 photocatalyst, the rate of hydrogen evolution to absorbed dye is estimated ~ 9.07 H_2 /dye/h. However, Co/TiO_2 catalyst shows relatively very low production rate of accumulated H_2 (~ 37.67 $\mu\text{mol/g-catal/h}$) and O_2 (~ 12.6 $\mu\text{mol/g-catal/h}$) and no visible activity is observed on TiO_2 catalyst. Rh B-Co/TiO_2 catalyst is 6 times active than Co/TiO_2 catalyst in terms of water splitting under visible light.

The absorbed dye on Rh B-Co/TiO_2 catalyst was gradually desorbed and turned the solution to slightly red color of Rh B as a function of reaction time. Fig. 6 shows the comparative study of amount of accumulated H_2 and O_2 gas evolution and the amount of desorbed dye on Rh B-Co/TiO_2 in the reaction time. The amount of desorbed Rh B dye increased to $\sim 50\%$ after 3 h and $\sim 80\%$ after 7 h and then reach the plateau of the desorbed amount at around 80%. The accumulated H_2 and O_2 gas evolution gradually increases as increasing the reaction time, even though significant desorption of Rh B, as shown in Table 3. Interestingly, the H_2 gas evolution per the number of dye per hour is almost constant, ~ 9.07 H_2 /dye/h in the overall range of reaction time. This suggests that water splitting reaction may be facilitated by the remained $\sim 20\%$ Rh B (~ 5 $\mu\text{mol-Rh B/g-catal}$) which is close to Co atom. However, around 80% absorbed Rh B to Ti atom and far from Co atom may not involve in the photocatalytic reaction. This synergic effect between the Rh B and Co is crucial to proceed the water splitting reaction under visible light.

Table 2

Accumulated H_2 and O_2 gas evolution in the photocatalytic water splitting over TiO_2 , Co/TiO_2 and Rh B-Co/TiO_2 under visible light.

| Time (h) | TiO_2 (μmol) | | Co/TiO_2 (μmol) | | Rh B-Co/TiO_2 (μmol) | |
|----------|------------------------------------|--------------|---------------------------------------|--------------|--|--------------|
| | H_2 | O_2 | H_2 | O_2 | H_2 | O_2 |
| 1 | 0.10 | 0.1 | 0.5 | 0.25 | 7.7 | 21.3 |
| 2 | 0.10 | 0.1 | 1.02 | 0.31 | 16.7 | 60.9 |
| 4 | 0.103 | 0.1 | 2.6 | 1.4 | 30.2 | 78.7 |
| 6 | 0.11 | 0.1 | 5.2 | 2.7 | 49.9 | 109.4 |
| 8 | 0.11 | 0.1 | 9.6 | 5.3 | 79.6 | 122.5 |
| 10 | 0.114 | 0.1 | 13.2 | 8.1 | 132.0 | 148.5 |

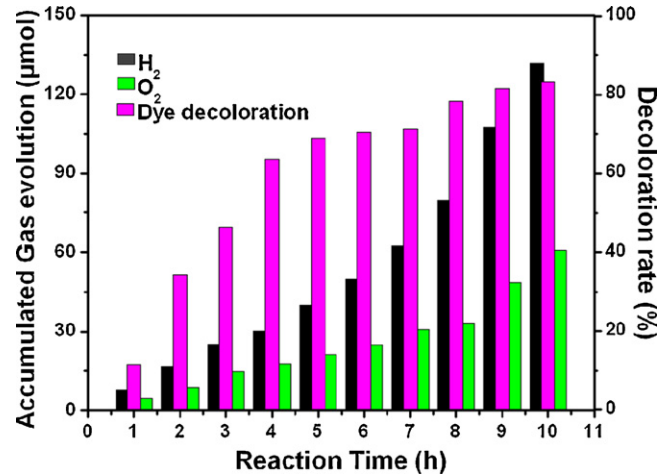


Fig. 6. Amount of accumulated hydrogen, oxygen evolution and desorption of Rh B dye as a function of reaction time.

Fig. 4(b) exhibits the Raman spectra of Co/TiO_2 and Rh B-Co/TiO_2 catalysts before and after reaction. All samples show the three Raman peaks in the range of 300 – 800 cm^{-1} that represent the typical crystal structure of TiO_2 materials. After the Rh B absorption, the intensity of Raman shift is decreased as compared to Co/TiO_2 , indicating the attachment of Rh B dye with Co/TiO_2 materials. The intensity of Raman shift is smaller than those of Rh B-Co/TiO_2 and Co/TiO_2 catalysts after water splitting reaction, which demonstrates the lowering in the crystallinity of Co/TiO_2 . It may due to the detachment of Rh B dye on the surface of Rh B-Co/TiO_2 . This result indicates the absorption of Rh B absorption over the surface of Co/TiO_2 promotes the photocatalytic water splitting reaction under visible light inspite of detachment of Rh B dye from the catalyst after reaction.

Rh B dye in Rh B-Co/TiO_2 photocatalytic improves the light harvesting of water splitting reaction as illustrated in Fig. 7. Under visible light illumination, the absorbed dye molecule directly

Table 3

Accumulated H_2 evolution and dye desorption (%) in the photocatalytic water splitting over the surface of Rh B-Co/TiO_2 catalysts.

| Reaction time (h) | Desorption of dye (%) | Accumulated H_2 (μmol) |
|-------------------|-----------------------|--|
| 1 | 3.6 | 7.7 |
| 2 | 11.5 | 16.7 |
| 4 | 39.5 | 30.2 |
| 6 | 63.6 | 49.9 |
| 8 | 78.3 | 79.6 |
| 10 | 83.1 | 132.0 |

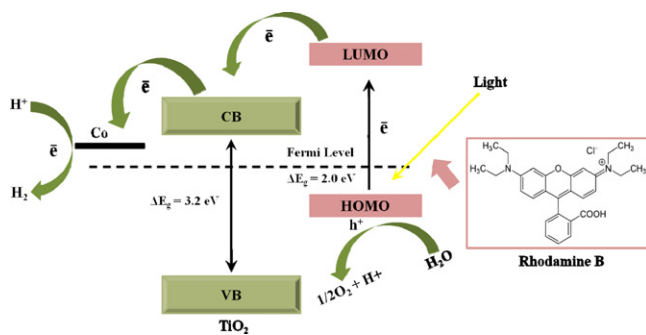


Fig. 7. The schematic illustration of water splitting over Rh B-Co/TiO₂ photocatalysts under visible light.

injects electron to Co metal as well as to the conduction band of TiO₂ and leaves the hydrogen and molecular oxygen radicals/ions at Co²⁺ ions which are closely related to better efficiency of hydrogen evolution. In case of Rh B-Co/TiO₂, the H₂ evolution is higher than Co/TiO₂ and TiO₂ due to the efficient electron transfer from dye to Co via TiO₂. It has been reported that noble metal loading into TiO₂ materials invokes absorption of dye and charge separation of e⁻-h⁺ pairs, which affects the performance of hydrogen evolution from H₂O due to the synergic effect [29,30]. Therefore, the prepared Co/TiO₂ catalysts may significantly increases the Rh B dye absorption and charge separation of e⁻-h⁺ pairs in Rh B-Co/TiO₂ catalyst, resulting in the high H₂ evolution as compared to Co/TiO₂ under visible light illumination as depicted in Fig. 6. In order to investigate the role of Co metal, a parallel study has been carried out for photocatalytic water splitting over only Rh B-TiO₂ catalyst under the visible light illumination. Hydrogen evolution is not detected on Rh B-TiO₂ catalyst. Moreover, it could expect that band gap energy of TiO₂ is not enough to transfer hole from the valance band to oxidized Rh B dye for the regeneration. Thus, the presence of Co²⁺ ions on surface of TiO₂ is crucial for facilitating electron transfer to the TiO₂ conduction band and downlift of valance band. Therefore, the Rh B-Co/TiO₂ may be increased the electron transfer and light harvesting efficiency during the water splitting under visible light, resulting in the high accumulated H₂ and O₂ evolution.

4. Conclusion

The sensitization of Rh B dye over the surface of Co/TiO₂ was carried out by simple physical absorption followed Co impregnation into TiO₂ materials for photocatalytic water splitting under visible light. The prepared Rh B-Co/TiO₂ materials showed a strong visible absorbance edge band in the range of 450–600 nm (max. absorbance at 550 nm) and slightly lowered band gap of 2.58 eV as compared to Co/TiO₂ (2.75 eV) and TiO₂ (3.21 eV). From photocatalytic water splitting results, Rh B-Co/TiO₂ catalysts showed the stoichiometric evolution of H₂ and O₂ gas of ~227.3 μmol/g-catal/h and ~98.9 μmol/g-catal/h, respectively, which was 6 times higher than that of H₂ evolution (~37.67 μmol/g-catal/h) with Co/TiO₂ catalysts. Interestingly, the accumulated H₂ and O₂ gas evolution was proportional to the water splitting reaction time even though continuous desorption of Rh B up to 80% after 8 h. However, the H₂

gas evolution per the number of dye per hour is almost constant, ~9.07 H₂/dye/h, in the overall range of reaction time. Conclusively, the water splitting reaction may be facilitated by the remained ~20% Rh B (~5 μmol-Rh B/g-catal) which may close to Co atom. Around 80% absorbed Rh B to Ti atom far from the Co atom may not involve in the photocatalytic reaction. This synergic effect between the Rh B and Co is crucial to enhance the water splitting reaction.

Acknowledgements

We gratefully acknowledge the support from the Ministry of Knowledge Economy and Korea Institute of Energy Technology Evaluation and Planning (KETEP) by the program of "Advanced track for Si-based Solar Cell Materials and Devices (Project Number # 20104010100660)" and the National Research Foundation (NRF, Project No. # 2011-0029527), Korea. Authors thank for Raman analysis from the Korea Basic Science Institute (KBSI) – Jeonju branch in Chonbuk National University. Authors wish to thank Mr. Jong-Gyun Kang in the Centre for University Research Facility (CURF) for taking good quality TEM images.

References

- [1] D. Sperling, J.S. Cannon, *The Hydrogen Energy Transition: Moving Toward the Post-petroleum Age in Transportation*, Elsevier Academic Press, London, 2004.
- [2] R. Kothari, D. Buddhi, R.L. Sawhney, *Renew. Sust. Energy Rev.* 12 (2008) 553.
- [3] M. Ni, M.K.H. Leung, D.Y.C. Leung, K. Sumathy, *Proceedings of the International Hydrogen Energy Forum* 1, 25–28 May, Beijing, PR China, 2004, pp. 475–480.
- [4] A. Kudo, *Int. J. Hydrogen Energy* 32 (2007) 2673.
- [5] K. Domen, A. Kudo, T. Onishi, *J. Catal.* 102 (1986) 92.
- [6] K. Maeda, K. Teramura, D. Lu, T. Takata, N. Saito, Y. Inoue, K. Domen, *Nature* 440 (2006) 295.
- [7] W.-W. So, K.J. Kim, S.J. Mon, *Int. J. Hydrogen Energy* 29 (2004) 229.
- [8] J.S. Jang, W. Li, S.H. Oh, J.S. Lee, *Chem. Phys. Lett.* 435 (2006) 278.
- [9] X.Z. Li, F.B. Li, C.L. Yang, W.K. Ge, *J. Photochem. Photobiol. A: Chem.* 141 (2001) 209.
- [10] A. Korzhak, N. Ermokhina, A. Stroyuk, V. Bukhtiyarov, A. Raevskaya, V. Litvin, *J. Photochem. Photobiol. A: Chem.* 198 (2008) 126.
- [11] M.A. Khan, M.S. Akhtar, S.I. Woo, O.-B. Yang, *Catal. Commun.* 10 (2008) 1.
- [12] (a) R. Abe, K. Sayama, H. Arakawa, *J. Photochem. Photobiol. A: Chem.* 166 (2004) 115;
(b) J. Ma, L.-S. Qiang, H.-Y. Li, X.-B. Tang, *Sci. Adv. Mater.* 2 (2010) 539.
- [13] K. Sayama, K. Mukasa, R. Abe, H. Arakawa, *Chem. Commun.* (2001) 2416.
- [14] (a) J.M. Stipkala, F.N. Castellano, T.A. Heimer, C.A. Kelly, K.J.T. Livi, G. Meyer, *J. Chem. Mater.* 9 (1997) 2341;
(b) J. Thomas, K.P. Kumar, S. Mathew, *Sci. Adv. Mater.* 3 (2011) 59.
- [15] A. Kudo, K. Domen, K. Maruya, K. Aika, T. Onishi, *J. Catal.* 111 (1988) 67.
- [16] Z. Jin, X. Zhang, Y. Li, S. Li, G. Lu, *Catal. Commun.* 8 (2007) 1267.
- [17] T. Peng, D. Ke, P. Cai, K. Dai, L. Ma, L. Zan, *J. Power Sources* 180 (2008) 498.
- [18] H. Misawa, H. Sakuragi, Y. Usui, K. Tokumaru, *Chem. Lett.* (1983) 1021.
- [19] T. Kajiwara, K. Hashimoto, T. Kawai, T. Sakata, *J. Phys. Chem.* 86 (1982) 709.
- [20] (a) M. Subramanian, S. Vijayalakshmi, S. Venkataraj, R. Jayavel, *Thin Solid Films* 516 (2008) 3776;
(b) T. Shimizu, T. Iyoda, Y. Koide, *J. Am. Chem. Soc.* 107 (1985) 35.
- [21] R. Abe, K. Hara, K. Sayama, K. Domen, H. Arakawa, *J. Photochem. Photobiol. A: Chem.* 137 (2000) 63.
- [22] J. Bandara, C.P. Uda Watta, C.S.K. Rajapakse, *Photochem. Photobiol. Sci.* 4 (2005) 857.
- [23] Z. Jin, X. Zhang, Y. Li, S. Li, G. Lu, *Catal. Commun.* 8 (2007) 1267.
- [24] M.L. Cui, J. Zhu, X.Y. Zhong, Y.G. Zhao, X.F. Duan, *Appl. Phys. Lett.* 85 (2004) 1698.
- [25] E.H. Poniatowski, S.V. -Munoz, R.A. -Murillo, R.R. -Talavera, R. Diamant, *Mater. Res. Bull.* 31 (1996) 329.
- [26] M.A. Khan, O.-B. Yang., *Catal. Today* 146 (2009) 177.
- [27] J.D. Lee, *Concise Inorganic Chemistry*, 166, 5th ed., John Wiley and Sons, 1996.
- [28] N. Dubey, K. Labhsetwar, S. Devotta, S. Rayalu, *Catal. Today* 129 (2007) 428.
- [29] H. Tada, K. Teranishi, Y. Inubushi, S. Ito, *Chem. Commun.* (1998) 2345.
- [30] R.I. Bickley, in: M. Schiavello (Ed.), *Heterogeneous Photocatalysis*, John Wiley & Sons, Chichester, 1997, p. 87.